

RESEARCH ARTICLE

Murine precursors to type 1 conventional dendritic cells induce tumor cytotoxicity and exhibit activated PD-1/PD-L1 pathway

Megan S. Molina^{1,2}, Emely A. Hoffman¹, Jessica Stokes¹, Nicole Kummet^{1,3}, Richard J. Simpson^{1,2,4,5}, Emmanuel Katsanis^{1,2,5,6,7*}

1 Department of Pediatrics, University of Arizona, Tucson, Arizona, United States of America, **2** Department of Immunobiology, University of Arizona, Tucson, Arizona, United States of America, **3** Department of Molecular and Cellular Biology, University of Arizona, Tucson, Arizona, United States of America, **4** Department of Nutritional Sciences, University of Arizona, Tucson, Arizona, United States of America, **5** The University of Arizona Cancer Center, Tucson, Arizona, United States of America, **6** Department of Medicine, University of Arizona, Tucson, Arizona, United States of America, **7** Department of Pathology, University of Arizona, Tucson, Arizona, United States of America

* ekatsani@arizona.edu



OPEN ACCESS

Citation: Molina MS, Hoffman EA, Stokes J, Kummet N, Simpson RJ, Katsanis E (2022) Murine precursors to type 1 conventional dendritic cells induce tumor cytotoxicity and exhibit activated PD-1/PD-L1 pathway. *PLoS ONE* 17(8): e0273075. <https://doi.org/10.1371/journal.pone.0273075>

Editor: Senthilnathan Palaniyandi, University of Missouri, UNITED STATES

Received: August 17, 2021

Accepted: August 2, 2022

Published: August 18, 2022

Peer Review History: PLOS recognizes the benefits of transparency in the peer review process; therefore, we enable the publication of all of the content of peer review and author responses alongside final, published articles. The editorial history of this article is available here: <https://doi.org/10.1371/journal.pone.0273075>

Copyright: © 2022 Molina et al. This is an open access article distributed under the terms of the [Creative Commons Attribution License](https://creativecommons.org/licenses/by/4.0/), which permits unrestricted use, distribution, and reproduction in any medium, provided the original author and source are credited.

Data Availability Statement: RNA sequencing data have been deposited to the UA Research Data Repository reDATA and are publicly available at the

Abstract

The immediate precursor to murine type 1 conventional DCs (cDC1s) has recently been established and named “pre-cDC1s”. Mature CD8 α + cDC1s are recognized for suppressing graft-versus-host disease (GvHD) while promoting graft-versus-leukemia (GvL), however pre-cDC1s have not previously been investigated in the context of alloreactivity or anti-tumor responses. Characterization of pre-cDC1s, compared to CD8 α + cDC1s, found that a lower percentage of pre-cDC1s express PD-L1, yet express greater PD-L1 by MFI and a greater percent PIR-B, a GvHD-suppressing molecule. Functional assays were performed *ex vivo* following *in vivo* depletion of CD8 α + DCs to examine whether pre-cDC1s play a redundant role in alloreactivity. Proliferation assays revealed less allogeneic T-cell proliferation in the absence of CD8 α + cDC1s, with slightly greater CD8+ T-cell proliferation. Further, in the absence of CD8 α + cDC1s, stimulated CD8+ T-cells exhibited significantly less PD-1 expression compared to CD4+ T-cells, and alloreactive T-cell death was significantly lower, driven by reduced CD4+ T-cell death. Tumor-killing assays revealed that T-cells primed with CD8 α -depleted DCs *ex vivo* induce greater killing of A20 B-cell leukemia cells, particularly when antigen (Ag) is limited. Bulk RNA sequencing revealed distinct transcriptional programs of these DCs, with pre-cDC1s exhibiting activated PD-1/PD-L1 signaling compared to CD8 α + cDC1s. These results indicate distinct T-cell-priming capabilities of murine pre-cDC1s compared to CD8 α + cDC1s *ex vivo*, with potentially clinically relevant implications in suppressing GvHD while promoting GvL responses, highlighting the need for greater investigation of murine pre-cDC1s.

following DOI: <https://doi.org/10.25422/azu.data.14241902>.

Funding: E.K. received funding from PANDA (<https://www.azpanda.org/>), Courtney's Courage (<https://teeupfortots.org/>), and Hyundai Hope on Wheels (<https://hyundaihopeonwheels.org/>). The funders had no role in study design, data collection and analysis, decision to publish, or preparation of the manuscript.

Competing interests: The authors have declared that no competing interests exist.

Introduction

A distinct murine dendritic cell (DC) has been identified as the immediate precursor to CD8 α + type 1 conventional DCs (cDC1s), termed “pre-cDC1”, phenotypically classified as CD24^{high}CD8 α - [1–5]. Pre-cDC1s become committed to the cDC1 lineage in the bone marrow (BM), and migrate out to the periphery where they acquire tissue-specific signals for their maturation into terminally differentiated CD8 α + or CD103+ cDC1s [1, 6–9]. Outside of their differential expression of CD24 and CD8 α , pre-cDC1s express the same pattern recognition receptors (PRRs) and other receptors as mature cDC1s (TLR3, DNGR1, Xcr1, etc.) [4, 10–14]. CD24 is a membrane glycoprotein that senses damage-associated molecular patterns (DAMPs), whereas CD8 α does not have any identified function [15, 16]. The expression levels of antigen (Ag)-processing enzymes has been compared among DCs and their precursors in the BM and spleen and found that pre-cDCs in the BM express relatively high levels of proteases compared to mature cDCs, but lose this high expression once they migrate to the spleen [17].

Direct comparisons of the two DC subsets have been conducted in the context of viral infection due to the central role of mature CD8 α + cDC1s in cross-presentation and cross-priming of CD8+ T-cells for anti-viral responses. One study found that pre-cDC1s induce greater expansion of Ag-specific memory T-cells and are better at reducing viral load compared to CD8 α + cDC1s [10]. This effect was largely attributed to the longer lifespan of pre-cDC1s in lymphoid organs [10]. It has also been determined that pre-cDC1s are not as efficient at cross-presentation of necrotic, cell-associated material [5, 10]. Further, de Brito *et al.* reported that pre-cDC1s do not acquire co-stimulatory capacity upon uptake of necrotic cell material, but are still able to cross-present [5]. They also found that, following TLR9 activation with CpG, pre-cDC1s are superior to CD8 α + cDC1s in CD8+ T-cell cross-priming of viral Ag [5].

Aside from anti-viral CD8+ T-cell responses, CD8 α + cDC1s also play a seminal role in promoting anti-tumor CD8+ T-cell responses via cross-presentation and cross-priming. Further, in the context of hematopoietic cell transplantation (HCT) CD8 α + cDC1s are recognized as potent suppressors of graft-versus-host disease (GvHD) through their ability to induce clonal deletion of alloreactive donor T-cells [18]. To our knowledge, the role of pre-cDC1s in alloreactivity and GvHD, and in generating anti-tumor responses, has not been previously investigated, despite studies documenting their superior ability to cross-prime CD8+ T-cells compared to mature CD8 α + cDC1s [5, 10]. This represents a significant gap in the literature regarding DC function, plasticity, and development in the contexts of transplantation and cancer. Herein we first characterized expression levels of various activating and inhibiting co-stimulatory molecules on pre-cDC1s compared to CD8 α + cDC1s at steady state. We then used a CD8 α -depleting antibody to remove CD8 α + cDC1s *in vivo* and then determine pan-DC function in their absence *ex vivo* in the context of alloreactive T-cell stimulation and tumor-killing. Finally, we performed bulk RNA sequencing of cell-sorted pre-cDC1s compared to CD8 α + cDC1s to discern underlying functional differences between these DC subsets.

Materials and methods

Ethics statement

Mouse studies were carried out in strict accordance with the recommendations in the Guide for the Care and Use of Laboratory Animals of the National Institutes of Health. Protocols were approved by the Institutional Animal Care and Use Committee at the University of Arizona (IACUC #14–171).

Mice

All strains of mice used (BALB/c and C57BL/6) were age-matched 6-10-week-old females purchased from The Jackson Laboratory. Mice were housed in specific pathogen-free conditions and cared for according to the guidelines of the University of Arizona's Institutional Animal Care and Use Committee. The method of sacrifice used for these studies was carbon dioxide (CO₂) overdose, in accordance with IACUC-approved methods of providing rapid, painless, stress-free death.

Drug preparation and administration

The CD8 α -depleting antibody (2.43 mAb) (BioXCell, BE0061) was diluted in sterile saline for *in vivo* administration. BALB/c mice were injected with 200 μ g 2.43 mAb intraperitoneally on day -3 and day -1 relative to the start of the functional assay on day 0.

Pan-dendritic cell isolation

Spleens were collected from naïve BALB/c mice and single-cell suspensions were generated. Red blood cells were lysed using Pharm Lyse (BD Biosciences). Splenocytes were washed in PBS (HyClone) and then Pan-DCs were isolated using the Pan-DC Isolation Kit (Miltenyi Biotec). Absolute counts were obtained using a hemocytometer and Trypan Blue.

Flow cytometry

Cells were washed in flow buffer (PBS with 0.5% FBS), incubated with anti-mouse Fc Block (Thermo Fisher Scientific), and flow cytometry was performed as previously reported [19–23]. All antibodies used for flow cytometry are listed in Table 1. T-cell death was determined using Propidium Iodide Ready Flow Reagent (Invitrogen). Fluorescence data were collected using an LSRFortessa cell analyzer (BD Biosciences) and analyzed using FlowJo 2 (Tree Star).

Table 1. Antibodies used for flow cytometry.

Antibody	Clone(s)	Vendor
Anti-mouse B220 Brilliant Violet 510	RA3-6B2	Biolegend
Anti-mouse CD4 APC/Cy7	GK1.5	Biolegend
Anti-mouse CD8 α PE-Cyanine7	53–6.7	Thermo Fisher
Anti-mouse CD11c FITC	N418	Miltenyi Biotec
Anti-mouse CD24 Pacific Blue	M1/69	Biolegend
Anti-mouse CD24 PE-Dazzle 594	M1/69	Biolegend
Anti-mouse CD25 AlexaFluor700	PC61	Biolegend
Anti-mouse CD69 PE/Cyanine5	H1.2F3	Thermo Fisher
Anti-mouse CD70 PerCP-eFluor710	FR70	Thermo Fisher
Anti-mouse H2Kb PerCP-eFluor 710	AF6-88.5.5.3	Thermo Fisher
Anti-mouse H2Kd PE	SF1-1.1.1	Thermo Fisher
Anti-mouse ICOS VioGreen	REA192	Miltenyi Biotec
Anti-mouse ICOSL PE	HK5.3	Biolegend
Anti-mouse PD-1 APC	29F.1A12	Biolegend
Anti-mouse PD-L1 PE/Dazzle594	10F.9G2	Biolegend
Anti-mouse PIR-B APC	10-1-PIR	Thermo Fisher
Anti-mouse TIM-3 PE	REA602	Miltenyi Biotec

<https://doi.org/10.1371/journal.pone.0273075.t001>

Mixed leukocyte reaction (MLR)

Splenic pan-DCs were isolated from the spleens of untreated or 2.43 mAb-treated BALB/c mice as described above. Some DCs were set aside to confirm CD8 α + cDC1 depletion by flow cytometry. Allogeneic T-cells were isolated from the spleens of naïve C57BL/6 mice using the Pan T-cell isolation kit II (Miltenyi Biotec). Purified T-cells were stained with CellTrace Violet (Invitrogen). Splenic DCs were co-cultured with allogeneic T-cells in proliferation assay media (PAM) (RPMI-1640, 10% FBS, 0.5% Sodium Pyruvate, 0.5% MEM, and 55 μ M BME) at a ratio of 1:5 and incubated at 37°C with 7.5% CO₂. T-cells were stimulated with CD3/CD28 Dyna-Beads (Thermo Fisher Scientific) as a positive control. After 16–24 hours, rIL-2 (PeproTech) was added to each well at a final concentration of 50 IU/mL. Flow cytometry was performed to determine DC composition on day 2 of co-culture. After 3–4 days of co-culture flow cytometry was performed. Data were analyzed using Modfit software (Verity Software House) to determine the proliferation index (PI) of H2K^b+ T-cells.

Tumor-killing assay

A BALB/c B-cell lymphoblastic leukemia cell line, A20-luciferase (A20-Luc), was provided by Dr. Xue-Zhong Yu, MD (Medical University of South Carolina) and has previously been used in murine BMT studies [20]. A20-luc was cultured in RPMI 1640 (Hyclone SH30027) with 10% FBS, MEM, sodium pyruvate (Hyclone SH30239), and 2 μ L/mL Zeocin (Gibco) at 37°C and 5% CO₂. This tumor-killing assay was performed according to previous reports [24] and optimized for our purposes. Splenic pan-DCs were isolated from the spleens of naïve or 2.43 mAb-treated BALB/c mice as described. Allogeneic T-cells were isolated from the spleens of naïve C57BL/6 mice using the Pan T-cell isolation kit II (Miltenyi Biotec). Splenic DCs were co-cultured with allogeneic T-cells in a 96-well U-bottom TC-treated plate at a ratio of 1:5 and incubated at 37°C with 7.5% CO₂.

On day 3 of co-culture 1x10⁵, 2x10⁵, or 4x10⁵ A20-Luc mouse (H2K^d+) B-cell lymphoma target cells were added to the respective wells and mixed well with the pipette. Tumor alone controls were added to wells containing a volume of media equivalent to that of the DC:T-cell cultures. The following day, on day 4, each individual well was harvested and transferred into a black, clear-bottom, flat-bottom 96-well plate. Immediately prior to imaging, 50 μ L of luciferin (GoldBio, LUCK) was added to all wells using a multi-channel pipette. Bioluminescence (BLI) was measured using LagoX (Special Instruments Imaging, Tucson, AZ) and quantified using Aura software (Verity). BLI was averaged for technical replicates. Specific killing was calculated as a percent of the tumor alone control at each respective tumor concentration.

FACS cell sorting

Splenic pan DCs were isolated from nine age-matched, female, littermate BALB/c mice and pooled per three mice for a total of three biological replicates. Pooled DCs were washed in flow buffer (PBS with 0.5% FBS), incubated with anti-mouse Fc Block (Thermo Fisher Scientific), and then stained with CD8 α PE-Cy7 (Thermo Fisher; clone: 53–6.7), and CD24 Pacific Blue (Biolegend; clone: M1/69). CD8 α + and pre-cDC1 (CD24^{high} CD8 α -) were sorted using FACS Aria III (BD).

RNA sequencing

All cell samples were stored in PBS and RNAlater (Thermo Fisher) at 4°C prior to processing by the University of Arizona Genomics Core (UAGC). RNA Samples were assessed for quality with a High Sensitivity RNA Fragment Analyzer Kit (Advanced Analytics) and quantity with

an RNA HS assay kit (Qubit). Quality samples were used for library builds with the Rapid RNA Library Kit (Swift) and Dual Combinatorial Indexing Kit (Swift). Samples had quality and average fragment size assessed with the High Sensitivity NGS Analysis Kit (Advanced Analytics). Quantity was assessed with the Kapa Library Quantification kit (Illumina), and then samples were equimolar-pooled and clustered for sequencing using Illumina NextSeq500 run chemistry (NextSeq 500/550 High Output v2 kit 150 cycles). Data were sent to UAGC Bio-computing Group for further analysis.

Informatics

Paired-end reads were demultiplexed using Illumina's BaseSpace service. Reads were trimmed using Trimmomatic version 0.32 (USADelLab). Fastq files were aligned to the GRCm38 version of the mouse reference genome using STAR version 2.5.2b [25]. Gene level quantification was performed using htseq-count version 0.6.1 [26]. DESeq2 was used to conduct differential expression analysis with genes having an adjusted p-value (padj) < 0.05 being considered significant [27]. Pathway enrichment was performed on the significant DEGs using QIAGEN's IPA software tool. P value = 0.05 corresponds to a 1.3 -log p-value and is considered statistically significant. Gene expression patterns of molecules for each identified pathway were used to determine a z-score, with a z-score >2 meaning "activated" and a z-score <-2 meaning "inhibited". RNA sequencing data have been deposited to the UA Research Data Repository reDATA and are publicly available (<https://doi.org/10.25422/azu.data.14241902>).

Statistical analysis

Unpaired t-tests were used to determine significance between absolute counts, percent, MFI expression, and proliferation indices. Two-way ANOVA tests and Šidák's multiple comparisons tests were used to determine significance in CD8 α + cDC1 and pre-cDC1. Ordinary One-way ANOVA tests and Tukey's multiple comparisons tests were used to determine significance in percent specific killing of A20-Luc. P values <0.05 were considered statistically significant.

Results

Pre-cDC1s differ from CD8 α + cDC1s in their steady-state expression of co-stimulatory and co-inhibitory molecules

Splenic pan DCs were isolated from naïve mice and phenotypically characterized by flow cytometry. Pre-cDC1s are less abundant than CD8 α + cDC1s in the spleens of BALB/c mice (Fig 1A and 1B). Pre-cDC1s and CD8 α + cDC1s have been reported to express all the same PRRs and receptors for dead cell-associated Ag, and to have the same cross-presentation capabilities [10]. We first sought to determine the surface expression levels of various activating and inhibiting co-stimulatory molecules on the two DC subsets at steady state to confer potential differences in how they may stimulate adaptive T-cell responses. Compared to CD8 α + cDC1s, a lower percentage of pre-cDC1s express PD-L1 while those positively expressing PD-L1 have a higher MFI (Fig 1C). Notably, CD8+ cDC1s appear to have PD-L1^{high} and PD-L1^{dim} populations, whereas PD-L1-expressing pre-cDC1s primarily fall within the PD-L1^{high} population, with relatively fewer PD-L1^{dim} pre-cDC1s. Pre-cDC1s exhibit significantly greater percent expression of PIR-B (Fig 1D), a co-inhibitory molecule that suppresses lethal GvHD [28]. Regarding activating co-stimulatory molecules, pre-cDC1s express lower percent CD70 (Fig 1E), and greater percent ICOS-L (Fig 1F), with no differences in MFI. These data demonstrate that pre-cDC1s and CD8 α + cDC1s differ in their expression of various activating and inhibiting co-stimulatory molecules. While it is unclear whether the

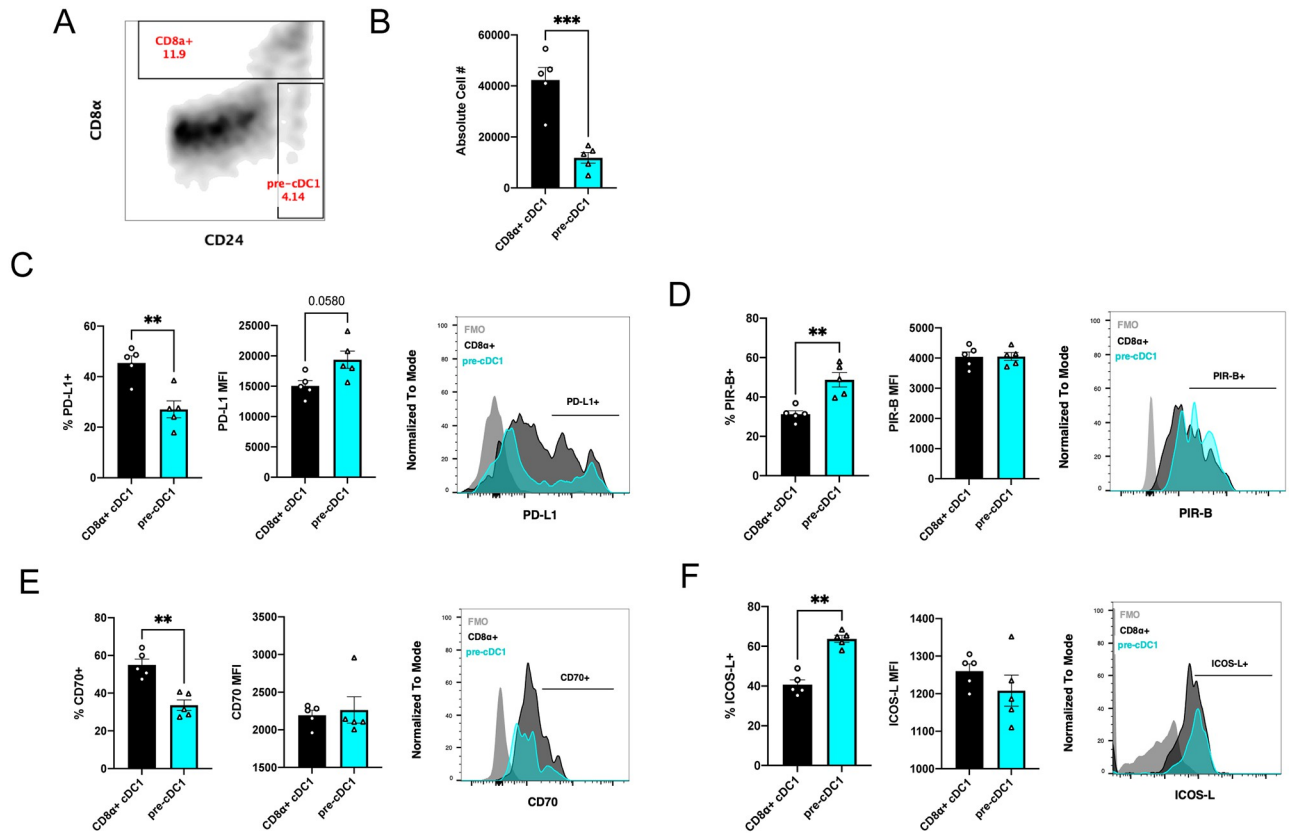


Fig 1. Pre-cDC1s differ from CD8α+ cDC1s in their steady-state expression of co-stimulatory and co-inhibitory molecules. Splenic pan DCs were isolated from naïve BALB/c mice and analyzed by flow cytometry to characterize pre-cDC1s and CD8α+ cDC1s. (A) Representative flow plot demonstrating gating strategy. Gated on CD11c+B220- (conventional DCs); pre-cDC1s are gated as CD24^{high}CD8α- and CD8α+ cDC1s are gated as CD8α+. (B) Mean absolute cell number of respective DC subsets shown with SEM. (C-F) Mean percent and MFI with representative histograms shown with SEM for expression of (C) PD-L1, (D) PIR-B, (E) CD70, and (F) ICOSL on CD8α+ cDC1s (black) and pre-cDC1s (cyan). Data is representative of two experiments. (n = 5 per group). Paired t tests were used to determine significance between DC subsets. **P<0.01, ***P<0.001.

<https://doi.org/10.1371/journal.pone.0273075.g001>

expression pattern of pre-cDC1s results in a net function that is more immunogenic or tolerogenic compared to CD8α+ cDC1s, these results suggest potential differences in T-cell effector function modulation by these DC subsets following the same antigenic stimulus.

Using a CD8α-depleting antibody to test functional redundancy

We next sought to compare the functions of pre-cDC1s and CD8α+ cDC1s. Unfortunately, there are no suitable mouse models commercially available that would allow us to properly investigate the separate functions of these DC subsets. The extreme rarity of these two DC populations complicate their examination *in vivo* and make cell-sorting for *ex vivo* assays unfeasible. Since the differentiating feature of these subsets is expression of CD8α, we used a CD8α-depleting antibody (2.43 mAb) to remove CD8α+ cDC1s *in vivo*. Depletion was confirmed by flow cytometry of splenocytes harvested from mice receiving CD8α-depleting antibody compared to untreated mice (Fig 2A and 2B). As previously reported, depletion of CD8α+ cDC1s also resulted in an increase in the proportion and absolute number of pre-cDC1s (Fig 2B and 2C) [10]. This strategy allowed us to evaluate splenic DC function in the presence and absence of CD8α+ cDC1s to determine whether pre-cDC1s exhibit functional redundancy. We therefore proceeded with the *ex vivo* proliferation assay outlined in the schematic in Fig 2D.

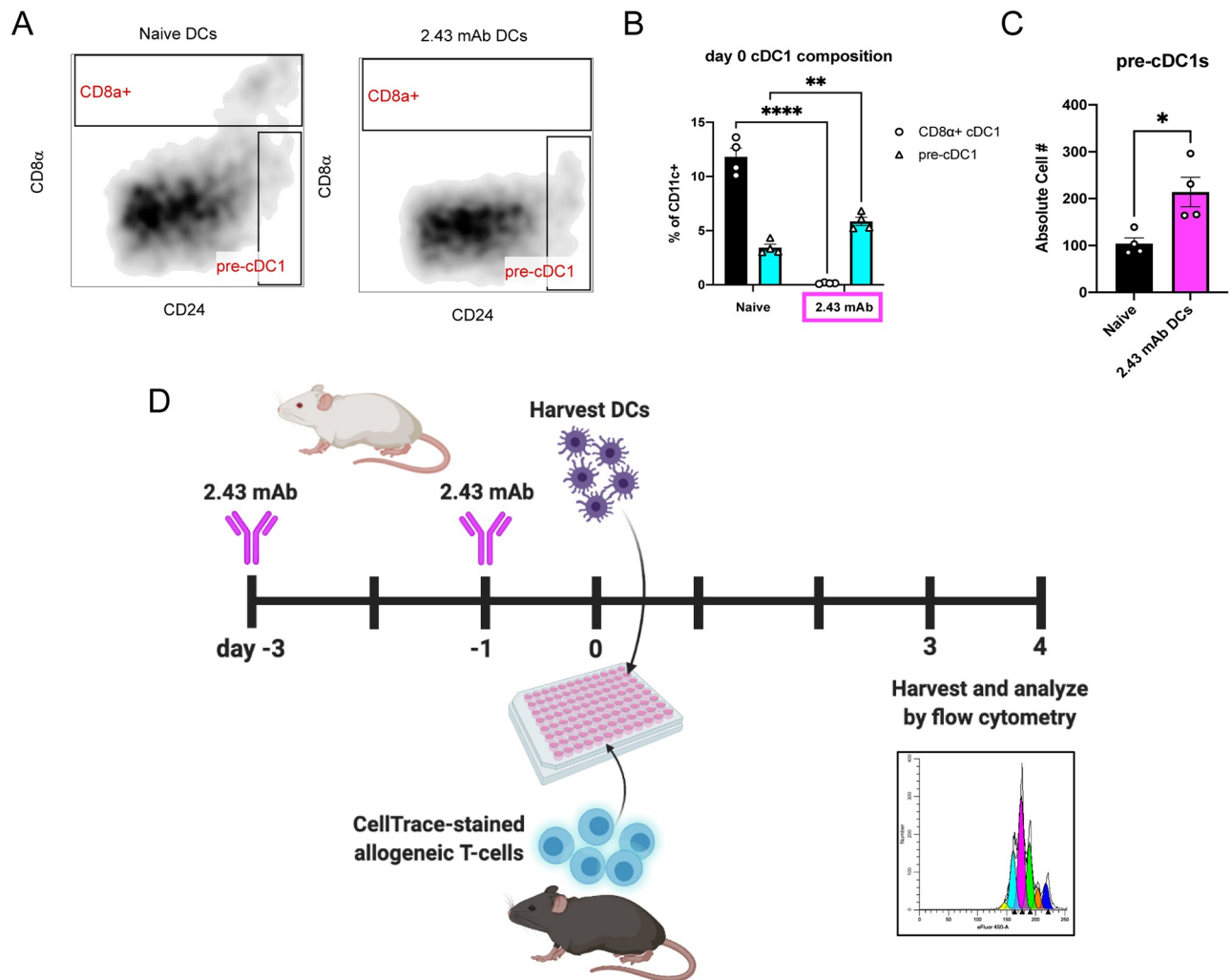


Fig 2. Using a CD8 α -depleting antibody to determine functional redundancy. BALB/c mice were dosed with 200 μ g of 2.43 mAb antibody intraperitoneally on day -3 and day -1. On day 0, splenic DCs were isolated and analyzed by flow cytometry. Data is representative of three independent experiments. (n = 4 per group) (A) Representative flow plots depicting relative cDC1 proportions in naïve DCs (left) and 2.43 mAb DCs (right). Gated on CD11c+B220- (conventional DCs). (B) Mean percent of CD8 α + cDC1s (black) and pre-cDC1s (cyan) in untreated and 2.43 mAb-treated DCs shown with SEM. Two-way ANOVA and Dunnett's multiple comparisons used to determine significance. **P<0.01, ****P<0.0001. (C) Mean absolute cell number of pre-cDC1s (CD24^{high}CD8 α -) in untreated (black) and 2.43 mAb-treated (magenta) groups shown with SEM. Unpaired t test used to determine significance. *P<0.05. (D) Schematic depicting experimental design for proposed allogeneic mixed leukocyte reaction (MLR) using 2.43 mAb treatment.

<https://doi.org/10.1371/journal.pone.0273075.g002>

2.43 mAb-treated DCs induce less proliferation, altered PD-1 expression, and depressed induction of cell death of alloreactive T-cells

We first sought to compare the ability of 2.43 mAb-treated DCs to stimulate alloreactive T-cell proliferation using an *ex vivo* allogeneic MLR. Using ModFit software, we first gated on H2K^b+ cells to distinguish T-cells, then fit the parent peak using each corresponding T-cell alone control and generated the representative CellTrace dilution histograms for each experimental condition and timepoint (Fig 3A). ModFit software calculates a proliferation index (PI) based on the area under the curves representing consecutive cell divisions. We found that 2.43 mAb-treated DCs induced significantly less alloreactive T-cell proliferation on day 3 (Fig

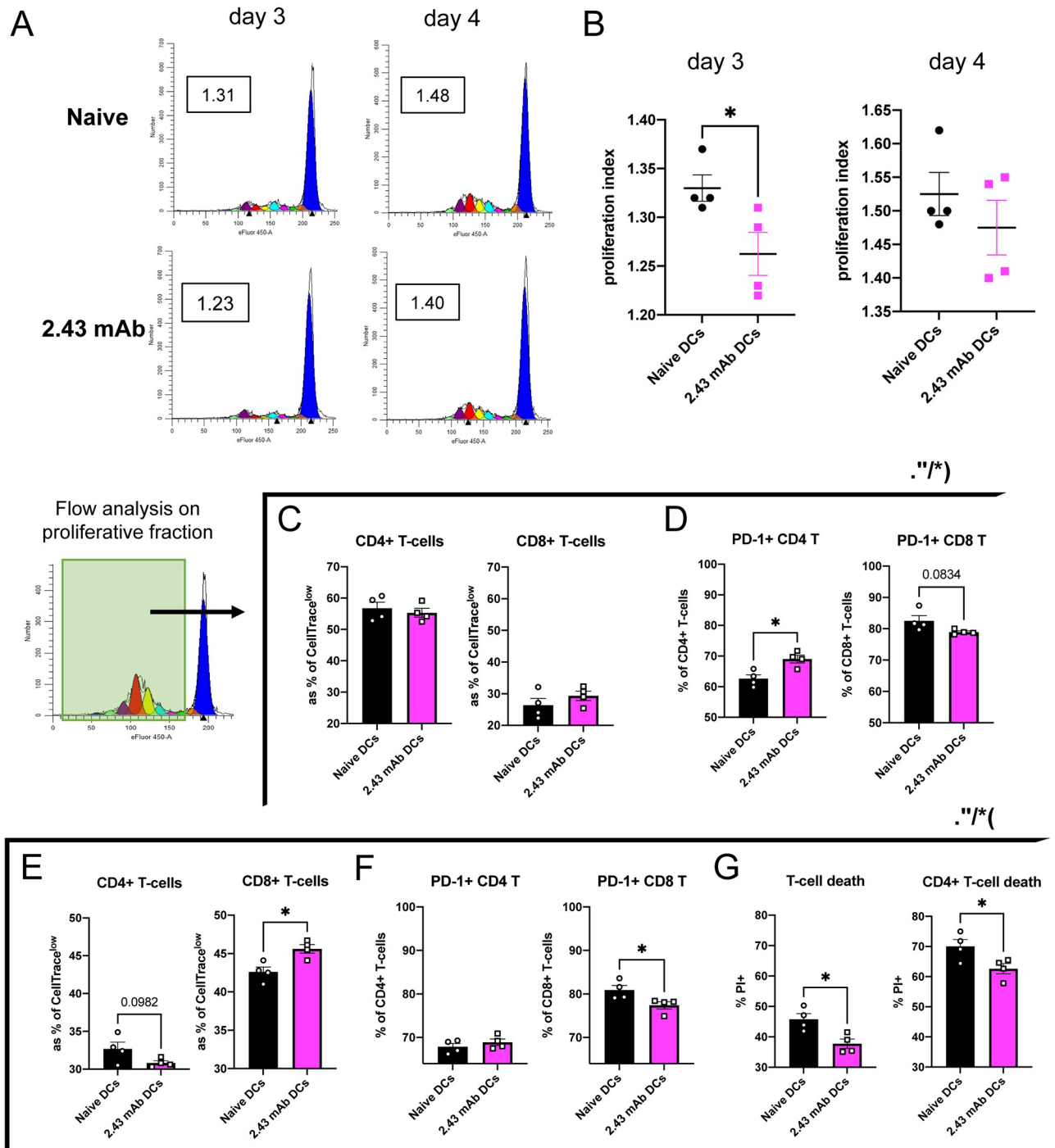


Fig 3. 2.43 mAb-treated DCs induce less proliferation, altered PD-1 expression, and depressed induction of cell death of alloreactive T-cells. BALB/c mice were dosed with 200 μ g of 2.43 mAb antibody intraperitoneally on day -3 and day -1. On day 0, splenic DCs were isolated and plated in an allogeneic MLR. Alloreactive T-cell proliferation was assessed on day 3 and day 4 of co-culture. Data is representative of two independent experiments. (n = 4 per group) (A-B) ModFit Software analysis of CellTrace dye dilutions. (A) Representative histograms depicting proliferation of H2K^b T-cells following stimulation with naïve DCs (top) or 2.43 mAb DCs (bottom) on days 3 and 4. Proliferation Index (PI) for representative histograms is boxed. (B) Mean PI for naïve or 2.43 mAb DCs shown with SEM. (C-G) Flow analysis of the proliferative fraction of T-cells was determined by first gating on H2K^b CellTrace^{low} T-cells. (C) Mean percent of proliferated T-cells that are CD4+ (left) and CD8+ (right) on day 3 shown with SEM. (D) Mean percent of proliferated CD4+ (left) and CD8+ (right) T-cells expressing PD-1 on day 3 shown with SEM. (E) Mean percent of proliferated T-cells that are CD4+ (left) and CD8+ (right) on day 4 shown with SEM. (F) Mean percent of proliferated CD4+ (left) and CD8+ (right) T-cells expressing PD-1 on day 4 shown with SEM. (G) Mean percent of proliferated T-cells (left) and CD4+ T-cells (right) that are Propidium Iodide+ shown with SEM. Unpaired t tests were used to determine significance between groups. *P<0.05.

<https://doi.org/10.1371/journal.pone.0273075.g003>

3B), though by day 4 this was no longer significant. We also characterized the proliferative fraction of T-cells via flow cytometry by first gating on H2K^b+CellTrace^{low} T-cells. On day 3 of the assay, we observed more CD4+ T-cell proliferation compared to CD8+ T-cell proliferation in both naïve and 2.43 mAb-treated conditions (Fig 3C). We further evaluated their expression of various surface markers of T-cell activation, exhaustion, and anergy. We found that on day 3, 2.43 mAb-treated DCs induced significantly greater expression of PD-1 on CD4+ T-cells and trended toward less expression on CD8+ T-cells, compared to untreated DCs (Fig 3D). Analysis of the proliferative fraction of T-cells was performed on day 4 of the assay and found that 2.43 mAb-treated DCs resulted in greater representation of CD8+ T-cells within the proliferative fraction (Fig 3E). We additionally found that among proliferated CD8+ T-cells, significantly fewer of them expressed PD-1 (Fig 3F). On day 4 we assessed induction of alloreactive T-cell death, a reported function of CD8 α + cDC1s, and found that 2.43 mAb-treated DCs induced significantly less alloreactive T-cell death compared to untreated DCs, and this was primarily driven by reduced induction of CD4+ T-cell death (Fig 3G) [18, 29].

2.43 mAb-treated DCs retain a lower frequency of CD8 α + cDC1s in *ex vivo* cultures

We next wanted to know how long CD8 α + cDC1 depletion persisted *ex vivo* since pre-cDC1s may mature into CD8 α + cDC1s upon entering the spleen and receiving tissue-specific signals. We therefore analyzed DCs in untreated versus 2.43 mAb-treated conditions on day 2 of *ex vivo* co-culture with allogeneic T-cells, gating on H2K^d+CD11c+ cells to distinguish them (Fig 4A) and found a significantly lower frequency of H2K^d+CD11c+ DCs present in cultures on day 2 under 2.43 mAb-treated conditions (Fig 4B). We further assessed the composition of cDC1s as a percent of H2K^d+CD11c+ DCs (Fig 4C) and confirmed persistence of a significantly lower proportion of CD8 α + cDC1s in the 2.43 mAb-treated group compared to untreated (Fig 4D). These confounding factors of overall fewer DCs in culture and reduced proportion of CD8 α + cDC1s may contribute to the differential effects on T-cell proliferation, PD-1 expression, and induced cell death.

Depletion of CD8 α + cDC1s results in improved tumor-killing

We additionally sought to evaluate the ability of 2.43 mAb-treated DCs to induce anti-tumor responses. We plated naïve and 2.43 mAb DCs with allogeneic T-cells on day 0, added A20 mouse lymphoma cells transduced to express luciferase (A20-Luc) on day 3 of co-culture, and then measured bioluminescence (BLI) of A20-Luc tumor cells on day 4 (Fig 5A) [24]. A representative plate image depicts the BLI readout (Fig 5B). Tumor cytotoxicity was calculated as a percent of the tumor alone BLI for each tumor concentration. Our results demonstrate that 2.43 mAb-treated DCs resulted in induction of significantly higher killing of A20-Luc tumor cells compared to untreated DCs at tumor concentrations of 1×10^5 (Fig 5C) and 2×10^5 (Fig 5D). These data indicate that the depletion of CD8 α + cDC1s with 2.43 mAb can enhance DC-induced anti-leukemic cytotoxic activity despite having less alloreactive T-cell proliferation.

Pre-cDC1 and CD8 α + cDC1 exhibit distinct transcriptional programs

We finally wanted to determine whether murine pre-cDC1s and CD8 α + cDC1s differ transcriptionally. Bulk RNA sequencing of cell-sorted pre-cDC1s and CD8 α + cDC1s was performed with the help of the University of Arizona Genomics Core (UAGC). These data revealed significant differences in the expression of various transcripts, exemplified in a volcano plot (Fig 6A). Among the most significantly downregulated genes in pre-cDC1s compared to mature CD8 α + cDC1s are Tnfrsf4 (OX40), IL-12p40, and Cxcl11. OX40 expression

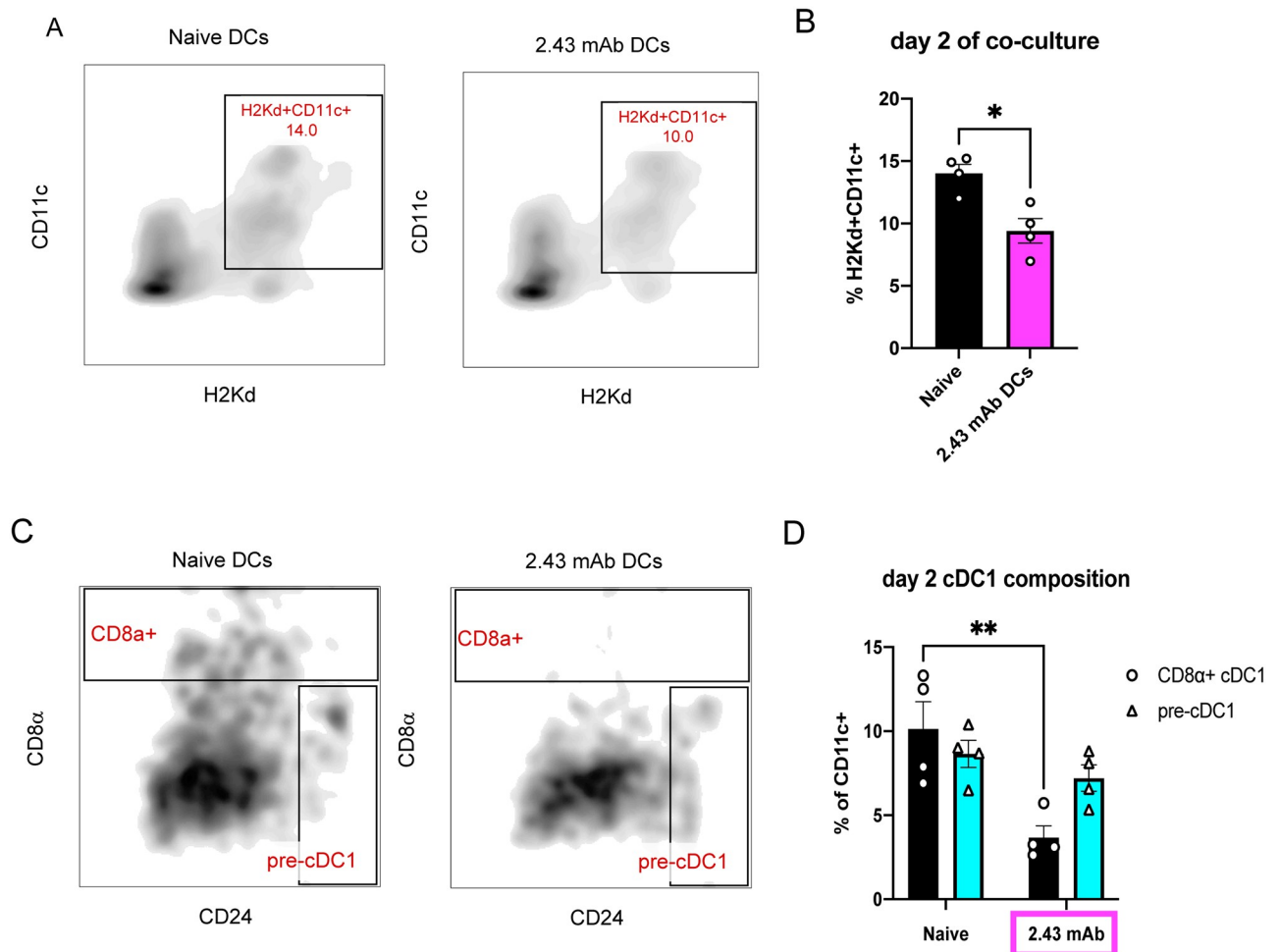


Fig 4. 2.43 mAb-treated DCs retain a lower frequency of CD8 α + cDC1s. BALB/c mice were dosed with 200 μ g of 2.43 mAb antibody intraperitoneally on day -3 and day -1. On day 0, splenic DCs were isolated and plated in an allogeneic MLR. DC composition was determined by flow cytometry on day 2 of co-culture. Data is representative of two independent experiments. (n = 4 per group) (A) Representative flow plots depicting percent of H2K^d+CD11c+ DCs in naïve DCs (left) and 2.43 mAb DCs (right) on day 2 of co-culture. (B) Mean percent of H2K^d+CD11c+ DCs for naïve (black) or 2.43 mAb DCs (magenta) shown with SEM. Unpaired t test was used to determine significance between groups. **P<0.01. (C) Representative flow plots depicting percent CD8 α + cDC1s and pre-cDC1s in naïve (left) and 2.43 mAb DCs (right). (D) Mean percent CD8 α + cDC1s (black bars) and pre-cDC1s (teal bars) in naïve and 2.43 mAb DCs shown with SEM. 2way ANOVA and Šidák's multiple comparison used to determine statistical significance. **P<0.01.

<https://doi.org/10.1371/journal.pone.0273075.g004>

on pDCs has been shown to promote anti-tumor immunity, however, to our knowledge, expression of OX40 on CD8 α + cDC1s has not been previously reported [30]. IL-12p40 and Cxcl11 are pro-inflammatory and support the recruitment of lymphocytes, so their downregulation may suggest that pre-cDC1 are less pro-inflammatory. Among the most significantly upregulated genes in pre-cDC1 are *Dram1*, *Dstn*, and several Ig variable transcripts thought to be involved in antigen binding. *Dram1* (DNA-damage-regulated autophagy modulator) regulates autophagy in part through effects on lysosomes and plays an important role in inducing selective autophagy in response to recognition of intracellular pathogens [31–33]. *Dstn* (Destrin) is a depolymerizing factor that enhances the turnover rate of actin, which plays a significant role in the capture and presentation of antigen [34].

Additionally, we find that pre-cDC1s differentially regulate several genes that are involved in Ag processing and presentation pathways. *Igkv7-33*, *Ighv1-12*, and *Igkv1-99* were all

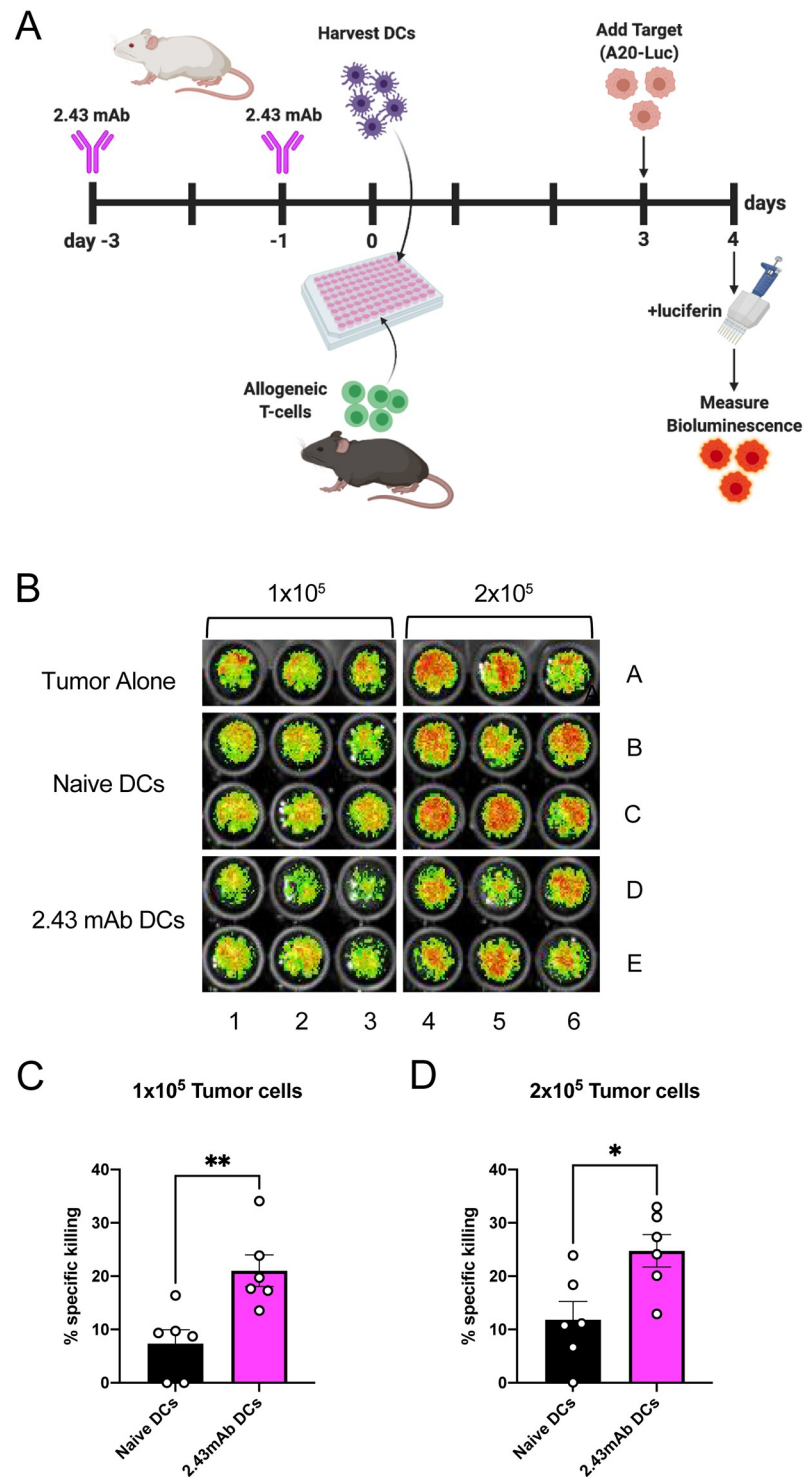


Fig 5. Depletion of CD8 α ⁺ cDC1s results in improved tumor-killing. BALB/c mice were dosed with 200 μ g of 2.43 mAb antibody intraperitoneally on day -3 and day -1. On day 0, splenic DCs were isolated and plated with allogeneic T-cells. On day 3 of co-culture A20-Luc tumor cells were added to wells at the indicated concentrations. On day 4, luciferin was added to wells and plates were imaged. BLI was measured for each independent well and averaged among technical replicates. BLI values were used to quantify specific killing as a percent of tumor alone control. Data is pooled from two independent experiments. (n = 6 per group) (A) Schematic depicting the experimental timeline. (B) Representative bioluminescence image depicting plate layout and showing BLI intensity on a scale from low (green) to high (red) indicative tumor burden. (C-D) Mean percent specific killing is shown with SEM for A20-Luc

concentrations of (C) 1×10^5 and (D) 2×10^5 A20-Luc tumor cells. Unpaired t test used to determine significance between groups. * $P < 0.05$, ** $P < 0.01$.

<https://doi.org/10.1371/journal.pone.0273075.g005>

significantly upregulated in pre-cDC1s and have vague roles in antigen binding and innate immune responses. Dstn (Destrin), an actin depolymerizing factor, was upregulated and contributes to the efficient capture and presentation of Ag [34]. Dram1 was upregulated and is associated with selective induction of autophagy [31]. Based on IPA results, mTOR signaling is predicted to be inhibited in pre-cDC1s compared to CD8 α + cDC1s, which has been linked to cytoprotective induction of autophagy [35]. Altogether, the RNAseq results suggest significant differences in how Ag processing and presentation, particularly with respect to autophagy, is regulated in pre-cDC1s compared to CD8 α + cDC1s at steady state.

Ingenuity pathway analysis (IPA) revealed a number of pathways predicted to be inhibited in pre-cDC1 compared to CD8 α + cDC1 including ICOS-ICOSL signaling, DC Maturation, and CD40 signaling (Fig 6B). These findings are in line with the activation state expected of immature, precursors to DCs [36]. Interestingly, we find that Flt3 signaling is also inhibited in pre-cDC1s compared to CD8 α + cDC1s, though it has been recently reported that Flt3L is dispensable for the final maturation step of cDC1s [37]. Pathways that were revealed to be activated in pre-cDC1s included several pathways regulating cell cycle control, oxidative phosphorylation, and the PD-1/PD-L1 cancer immunotherapy pathway (Fig 6C). Differentially activated cell cycle control may reflect the difference in lifespan of cDC1s compared to CD8 α + cDC1s [10]. A metabolic program favoring oxidative phosphorylation has been associated with tolerogenic DCs [38]. Predicted activation of the PD-1/PD-L1 pathway is interesting because we found that a smaller percentage of pre-cDC1s express PD-L1 compared to CD8 α + cDC1, but those pre-cDC1s that do positively express PD-L1 appear to express higher levels of it (Fig 1C). A heat map was generated for the PD-1/PD-L1 pathway and displays very clear differences in gene expression levels between pre-cDC1s and CD8 α + cDC1s (Fig 6D).

Discussion

The function of pre-cDC1s has not been extensively studied, in part because they have only recently been identified as the committed precursor to CD8 α + cDC1s [1, 4]. The few mechanistic reports that have directly compared the two DC subsets have determined that pre-cDC1s exhibit a significantly enhanced lifespan and induce greater expansion of Ag-specific memory CD8+ T-cells and control of viral load [5, 10]. There are still many gaps in our knowledge of how pre-cDC1s function as compared to CD8 α + cDC1s, as well as what factors trigger their immigration from the bone marrow to the spleen and maturation into CD8 α + cDC1s. Given the crucial role of CD8 α + cDC1s in suppressing GvHD while promoting GvL responses, the role of pre-cDC1s in induction of alloreactive T-cell responses and anti-tumor responses is of great clinical significance for HCT.

Our findings indicate that pre-cDC1s express significantly different levels of various co-signaling molecules compared to CD8 α + cDC1s. We observed that a significantly higher percentage of pre-cDC1s express PIR-B, which has been shown to regulate cytotoxic T-cell responses and prevent lethal GvHD, which would be advantageous in the HCT setting [27, 38, 39]. We also found that a lower percentage express PD-L1, which provides inhibitory signals to T-cells that can help mitigate GvHD [40–42]. Notably, CD8 α + cDC1s appear to have both PD-L1^{high} and PD-L1^{dim} populations, whereas positively expressing pre-cDC1s primarily fall into the PD-L1^{high} population. We additionally documented a significantly lower percentage of pre-cDC1s expressing CD70 compared to CD8 α + cDC1s. CD70 activates CD27 on T-cells which plays a nonredundant role in regulating T-cell, B-cell, and NK cell activity [43]. Studies have

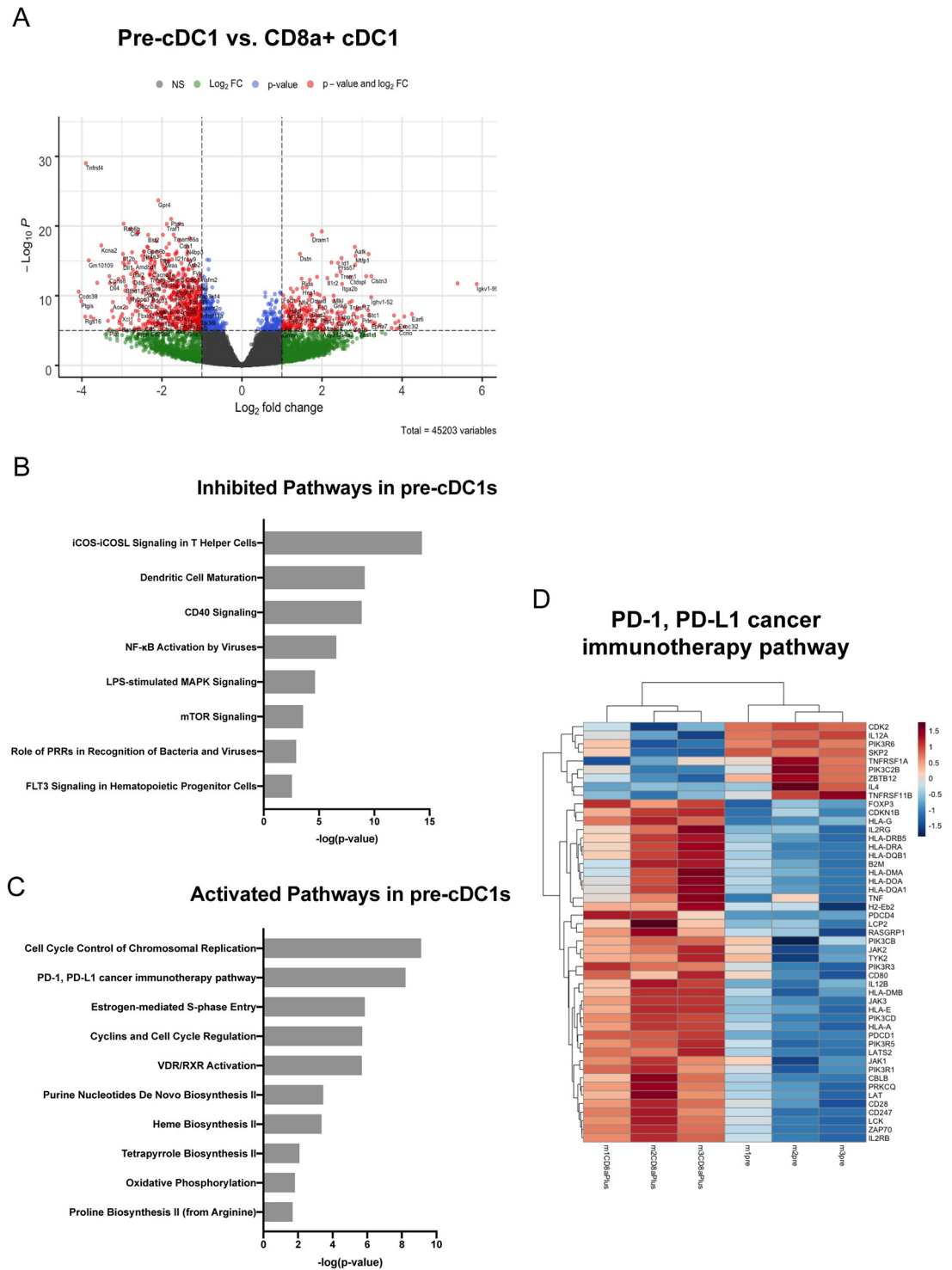


Fig 6. Pre-cDC1 and CD8α+ cDC1 exhibit distinct transcriptional programs. Splenic DCs were isolated from naïve BALB/c mice and pre-cDC1s and CD8α+ cDC1s were cell sorted for RNA sequencing. (A) Enhanced volcano plot identifying genes that are up or down-regulated in pre-cDC1s compared to CD8α+ cDC1s. (B-C) Pathway results using Qiagen’s IPA software. P = 0.05 corresponds to a 1.3 -log p-value, and anything above this value is considered statistically significant. (B) Pathways predicted to be significantly inhibited (z-score < -2) in pre-cDC1s compared to CD8α+ cDC1s. (C) Pathways predicted to be significantly activated (z-score < 2) in pre-cDC1s compared to CD8α+ cDC1s. (D) Heat map showing relative gene expression levels for the PD-1/PD-L1 cancer immunotherapy pathway. Full documentation, methodology, and raw data for this data set is available online at: <https://doi.org/10.25422/azu.data.14241902>.

<https://doi.org/10.1371/journal.pone.0273075.g006>

indicated that CD70 may prevent the induction of T-cell tolerance by steady state DCs, suggesting that lower expression by pre-cDC1s may be advantageous in HCT by promoting tolerance [44]. We also report that a significantly greater percentage of pre-cDC1s express ICOSL, which contributes to activation of T-cells and would therefore exacerbate GvHD [45]. This finding contradicts our RNAseq results which indicate that the ICOS-ICOSL signaling in T helper cells pathway is significantly inhibited in pre-cDC1s compared to CD8 α + cDC1s. Overall, these findings make it difficult to clearly ascertain the net effect of pre-cDC1s in inducing or protecting from GvHD when compared to CD8 α + cDC1s. A future line of work employing ICOS and ICOSL blockades would be helpful in delineating the role of this co-signaling molecule in the overall function of pre-cDC1s.

No mouse models currently exist that would allow us to adequately investigate the respective roles of pre-cDC1s and CD8 α + cDC1s without resulting in significant changes to other immune cell subsets. The extreme rarity of these DC subsets further complicates their investigation *in vivo*. We therefore examined the function of splenic pan-DCs *ex vivo* following *in vivo* treatment with an anti-CD8 α monoclonal antibody to deplete CD8 α + cDC1s, thereby indirectly assessing the role of CD8 α + cDC1s compared to pre-cDC1s. This imperfect approach for distinguishing the relative functions of pre-cDC1s and CD8 α + cDC1s has several caveats worth mentioning. First, in using a CD8 α -depleting antibody, we are depleting CD8+ T-cells in addition to CD8 α + cDC1s, which may have contributing effects on spleen cells and DCs specifically. Secondly, as others have shown, we find that depletion of CD8 α + cDC1s results in an increase in the percent and absolute number of pre-cDC1s in the spleen [5]. This was expected as we know that pre-cDC1s seed peripheral tissues from the BM in order to replenish mature CD8 α + cDC1s, however it may have unknown effects on splenic DC function. Newly seeded pre-cDC1s may behave differently compared to pre-cDC1s that have resided in the spleen longer. For instance, it has been demonstrated that pre-cDCs in the BM express very high levels of Ag processing enzymes and downregulate their expression upon migrating into peripheral tissues [17].

Allogeneic MLR results demonstrated that 2.43 mAb-treated DCs induce significantly less alloreactive T-cell proliferation *ex vivo* with a slight preference for proliferation of CD8+ T-cells over CD4+ T-cells. Moreover, 2.43 mAb-treated DCs resulted in greater expression of PD-1 on CD4+ T-cells, lower expression of PD-1 on CD8+ T-cells, as well as reduced cell death of CD4+ T-cells. Interpretation of these results is limited by the fact that 2.43 mAb depletion resulted in a lower percentage of H2K^d+CD11c+ cells on day 2 of culture in the MLR assays. The reason for this is unclear but suggests that 2.43 mAb-treated DCs did not persist as well *ex vivo* compared to untreated DCs, which would contribute to their observed decrease in inducing allogeneic T-cell proliferation. It is also possible that 2.43 mAb-treated DCs may be downregulating H2K^d or CD11c expression compared to untreated DCs. Nevertheless, evaluation of cDC composition of H2K^d+CD11c+ cells on day 2 of *ex vivo* culture demonstrated that 2.43 mAb-treated DCs maintained a predominant pre-cDC1 proportion over CD8 α + cDC1. Thus, we are confident that the differential T-cell responses observed are indicative of the relative abundance of pre-cDC1s and CD8 α + cDC1s.

Tumor killing assays revealed enhanced cytotoxicity against A20 B-cell lymphoblastic leukemia cell line induced by 2.43 mAb-treated DCs compared to untreated DCs, despite also having decreased stimulatory capacity of allogeneic T-cells. These findings suggest that 2.43 mAb-treated DCs may be skewed toward favoring GvL over GvHD. One would expect less alloreactive T-cell proliferation to translate to less tumor killing, though we cannot confirm from these studies whether or not tumor killing is T-cell-mediated. We also cannot rule out the possibility that 2.43 mAb-treated DCs are themselves cytotoxic. Reviewed by Larmonier *et al.* and Hanke *et al.*, DCs have been found to function as direct cytotoxic effectors against

tumor cells [46, 47]. This less conventional function of DCs has been found to be highly dependent upon NO synthase expression, peroxynitrites, and iNOS expression [48, 49]. Cytotoxic DC function has also been shown to be differentially regulated by PIAS-1 and STAT3 [50]. Furthermore, human DCs have also been shown to have cytotoxic function, also dependent upon peroxynitrites and restricted to immature DCs [51]. Future work is needed to investigate these mechanisms of cytotoxic function specifically in pre-cDC1s to determine whether they truly function as killer DCs.

RNAseq results comparing cell sorted pre-cDC1s and CD8 α + cDC1s reveal significant differences in the transcriptional programs of these DC subsets that have otherwise been thought of as having similar, if not identical, functions. Among the pathways predicted to be inhibited in pre-cDC1s include DC maturation, CD40 signaling, NF κ B activation, LPS-stimulated MAPK signaling, and the role of PRRs in recognition of bacteria and viruses. Overall, inhibition of these pathways is indicative an immature DC phenotype, which is unsurprising for a precursor DC but may also indicate a proclivity to induce tolerogenic responses. Additionally, the vitamin D VDR/RXR activation and oxidative phosphorylation pathways are predicted to be activated in pre-cDC1s and have both been linked to tolerogenic DC responses [38, 52]. The PD-1/PD-L1 is also predicted to be activated in pre-cDC1s compared to CD8 α + cDC1s, which would be highly beneficial for induction of tolerance in the HCT setting. Interestingly, while PD-1 signaling is critical to induction and maintenance of peripheral tolerance in transplantation, the induction of programmed cell death of alloreactive T-cells has been specifically linked to PD-L1, and its ligand is not believed to be PD-1 [53–57].

Given the more recent identification of pre-cDC1s, this DC subset has not been extensively studied in the contexts of alloreactivity and anti-tumor responses and genetically modified mouse models for investigating this rare cell type have not yet been developed. Limitations in our overall methodology make it difficult to make conclusions regarding the ability of pre-cDC1s to control allogeneic T-cell responses *in vivo*. Though, it is worth nothing that previous work from our laboratory has found a strong association between host pre-cDC1 abundance and improved survival from lethal GvHD in a major-mismatched bone marrow transplantation model [22]. Nevertheless, tumor-killing assays suggest that pre-cDC1s may support a vigorous cytotoxic response against leukemic cells *ex vivo*, particularly in the presence of limited Ag. Although a human equivalent of pre-cDC1s has not yet been identified, our understanding of human DC biology is changing very rapidly with sequencing technology [58–60]. Obtained RNA sequencing results suggest that these two DC populations are transcriptionally distinct. Given the highly conserved features of cDC1s between mice and humans, and the recent discovery of new DC subsets found in both species, it is plausible that humans express a “pre-cDC1” population as well [59, 61, 62].

In summary, pre-cDC1s exhibit significantly different expression patterns of various co-stimulatory molecules compared to CD8 α + cDC1s, suggesting that pre-cDC1s may induce different T effector responses than CD8 α + cDC1s when given the same antigenic stimulus. Our results also indicate that, in the absence of CD8 α + cDC1s, pre-cDC1s induce a more potent anti-tumor response in the presence of limited Ag. However, we may only speculate as to how pre-cDC1s function *in vivo*, and a better system is needed to more confidently and extensively investigate the role of pre-cDC1s in alloreactivity and anti-tumor responses. RNAseq results suggest an immature, tolerogenic function of pre-cDC1s and differential regulation of Ag processing and cross-presentation machinery. Altogether, these findings indicate a unique function of pre-cDC1s that warrants further investigation and consideration in future studies of anti-cancer responses and HCT using murine models.

Acknowledgments

The authors wish to thank Vanessa Frisinger for administrative assistance. We'd also like to thank the University of Arizona Flow Cytometry Core Facility for the use of their analytical software and facilities, as well as the University of Arizona Genomics Core Facility for processing and generation of RNAseq data and informatics expertise.

Author Contributions

Conceptualization: Megan S. Molina, Emely A. Hoffman, Jessica Stokes, Richard J. Simpson, Emmanuel Katsanis.

Data curation: Megan S. Molina, Emely A. Hoffman, Jessica Stokes, Nicole Kummet.

Formal analysis: Megan S. Molina.

Funding acquisition: Emmanuel Katsanis.

Investigation: Megan S. Molina.

Methodology: Megan S. Molina, Emely A. Hoffman, Jessica Stokes, Nicole Kummet.

Supervision: Emmanuel Katsanis.

Writing – original draft: Megan S. Molina.

Writing – review & editing: Megan S. Molina, Emely A. Hoffman, Jessica Stokes, Richard J. Simpson, Emmanuel Katsanis.

References

1. Schlitzer A., et al., Identification of cDC1- and cDC2-committed DC progenitors reveals early lineage priming at the common DC progenitor stage in the bone marrow. *Nat Immunol*, 2015. 16(7): p. 718–28. <https://doi.org/10.1038/ni.3200> PMID: 26054720
2. Guillemin M., et al., Dendritic cells, monocytes and macrophages: a unified nomenclature based on ontogeny. *Nat Rev Immunol*, 2014. 14(8): p. 571–8. <https://doi.org/10.1038/nri3712> PMID: 25033907
3. Grajales-Reyes G.E., et al., Batf3 maintains autoactivation of Irf8 for commitment of a CD8alpha(+) conventional DC clonogenic progenitor. *Nat Immunol*, 2015. 16(7): p. 708–17.
4. Cook S.J., et al., Differential chemokine receptor expression and usage by pre-cDC1 and pre-cDC2. *Immunol Cell Biol*, 2018. 96(10): p. 1131–1139. <https://doi.org/10.1111/imcb.12186> PMID: 29920767
5. de Brito C., et al., CpG promotes cross-presentation of dead cell-associated antigens by pre-CD8alpha + dendritic cells [corrected]. *J Immunol*, 2011. 186(3): p. 1503–11.
6. Diao J., et al., Characterization of distinct conventional and plasmacytoid dendritic cell-committed precursors in murine bone marrow. *J Immunol*, 2004. 173(3): p. 1826–33. <https://doi.org/10.4049/jimmunol.173.3.1826> PMID: 15265914
7. Naik S.H., et al., Intrasplenic steady-state dendritic cell precursors that are distinct from monocytes. *Nat Immunol*, 2006. 7(6): p. 663–71. <https://doi.org/10.1038/ni1340> PMID: 16680143
8. Liu K., et al., In vivo analysis of dendritic cell development and homeostasis. *Science*, 2009. 324(5925): p. 392–7. <https://doi.org/10.1126/science.1170540> PMID: 19286519
9. Ginhoux F., et al., The origin and development of nonlymphoid tissue CD103+ DCs. *J Exp Med*, 2009. 206(13): p. 3115–30. <https://doi.org/10.1084/jem.20091756> PMID: 20008528
10. Bedoui S., et al., Characterization of an immediate splenic precursor of CD8+ dendritic cells capable of inducing antiviral T cell responses. *J Immunol*, 2009. 182(7): p. 4200–7. <https://doi.org/10.4049/jimmunol.0802286> PMID: 19299718
11. Vremec D., et al., CD4 and CD8 expression by dendritic cell subtypes in mouse thymus and spleen. *J Immunol*, 2000. 164(6): p. 2978–86. <https://doi.org/10.4049/jimmunol.164.6.2978> PMID: 10706685
12. Belz G.T., et al., CD36 is differentially expressed by CD8+ splenic dendritic cells but is not required for cross-presentation in vivo. *J Immunol*, 2002. 168(12): p. 6066–70. <https://doi.org/10.4049/jimmunol.168.12.6066> PMID: 12055215

13. Anjuere F., et al., Definition of dendritic cell subpopulations present in the spleen, Peyer's patches, lymph nodes, and skin of the mouse. *Blood*, 1999. 93(2): p. 590–8. PMID: [9885220](#)
14. Lahoud M.H., et al., Signal regulatory protein molecules are differentially expressed by CD8- dendritic cells. *J Immunol*, 2006. 177(1): p. 372–82. <https://doi.org/10.4049/jimmunol.177.1.372> PMID: [16785533](#)
15. Kim T.S., et al., Distinct dendritic cell subsets dictate the fate decision between effector and memory CD8(+) T cell differentiation by a CD24-dependent mechanism. *Immunity*, 2014. 40(3): p. 400–13. <https://doi.org/10.1016/j.immuni.2014.02.004> PMID: [24631155](#)
16. Shortman K. and Heath W.R., The CD8+ dendritic cell subset. *Immunol Rev*, 2010. 234(1): p. 18–31. <https://doi.org/10.1111/j.0105-2896.2009.00870.x> PMID: [20193009](#)
17. Mahiddine K., et al., Tissue-Specific Factors Differentially Regulate the Expression of Antigen-Processing Enzymes During Dendritic Cell Ontogeny. *Front Immunol*, 2020. 11: p. 453. <https://doi.org/10.3389/fimmu.2020.00453> PMID: [32296417](#)
18. Markey K.A., et al., Flt-3L Expansion of Recipient CD8alpha(+) Dendritic Cells Deletes Alloreactive Donor T Cells and Represents an Alternative to Posttransplant Cyclophosphamide for the Prevention of GVHD. *Clin Cancer Res*, 2018. 24(7): p. 1604–1616.
19. Stokes J., et al., Post-transplant bendamustine reduces GvHD while preserving GvL in experimental haploidentical bone marrow transplantation. *Br J Haematol*, 2016. 174(1): p. 102–16. <https://doi.org/10.1111/bjh.14034> PMID: [27030315](#)
20. Stokes J., et al., Bendamustine with Total Body Irradiation Limits Murine Graft-versus-Host Disease in Part Through Effects on Myeloid-Derived Suppressor Cells. *Biol Blood Marrow Transplant*, 2019. 25(3): p. 405–416. <https://doi.org/10.1016/j.bbmt.2018.10.009> PMID: [30326280](#)
21. Stokes J., et al., Bendamustine with total body irradiation conditioning yields tolerant T-cells while preserving T-cell-dependent graft-versus-leukemia. *Oncoimmunology*, 2020. 9(1): p. 1758011. <https://doi.org/10.1080/2162402X.2020.1758011> PMID: [32391190](#)
22. Molina M.S., et al., Bendamustine Conditioning Skews Murine Host DCs Toward Pre-cDC1s and Reduces GvHD Independently of Batf3. *Front Immunol*, 2020. 11: p. 1410. <https://doi.org/10.3389/fimmu.2020.01410> PMID: [32765499](#)
23. Zeng Y., et al., Activated MHC-mismatched T helper-1 lymphocyte infusion enhances GvL with limited GvHD. *Bone Marrow Transplant*, 2014. 49(8): p. 1076–83. <https://doi.org/10.1038/bmt.2014.91> PMID: [24777185](#)
24. Mohammadpour H., et al., Blockade of Host beta2-Adrenergic Receptor Enhances Graft-versus-Tumor Effect through Modulating APCs. *J Immunol*, 2018. 200(7): p. 2479–2488.
25. Dobin A., et al., STAR: ultrafast universal RNA-seq aligner. *Bioinformatics*, 2013. 29(1): p. 15–21. <https://doi.org/10.1093/bioinformatics/bts635> PMID: [23104886](#)
26. Anders S., Pyl P.T., and Huber W., HTSeq—a Python framework to work with high-throughput sequencing data. *Bioinformatics*, 2015. 31(2): p. 166–9. <https://doi.org/10.1093/bioinformatics/btu638> PMID: [25260700](#)
27. Love M.I., Huber W., and Anders S., Moderated estimation of fold change and dispersion for RNA-seq data with DESeq2. *Genome Biol*, 2014. 15(12): p. 550. <https://doi.org/10.1186/s13059-014-0550-8> PMID: [25516281](#)
28. Scroggins S.M., et al., Characterization of regulatory dendritic cells that mitigate acute graft-versus-host disease in older mice following allogeneic bone marrow transplantation. *PLoS One*, 2013. 8(9): p. e75158. <https://doi.org/10.1371/journal.pone.0075158> PMID: [24040397](#)
29. Suss G. and Shortman K., A subclass of dendritic cells kills CD4 T cells via Fas/Fas-ligand-induced apoptosis. *J Exp Med*, 1996. 183(4): p. 1789–96. <https://doi.org/10.1084/jem.183.4.1789> PMID: [8666935](#)
30. Poropatich K., et al., OX40+ plasmacytoid dendritic cells in the tumor microenvironment promote antitumor immunity. *J Clin Invest*, 2020. 130(7): p. 3528–3542. <https://doi.org/10.1172/JCI131992> PMID: [32182225](#)
31. Guan J.J., et al., DRAM1 regulates apoptosis through increasing protein levels and lysosomal localization of BAX. *Cell Death Dis*, 2015. 6: p. e1624. <https://doi.org/10.1038/cddis.2014.546> PMID: [25633293](#)
32. van der Vaart M., et al., The DNA damage-regulated autophagy modulator DRAM1 links mycobacterial recognition via TLR-MYD88 to autophagic defense [corrected]. *Cell Host Microbe*, 2014. 15(6): p. 753–67. <https://doi.org/10.1016/j.chom.2014.05.005> PMID: [24922577](#)
33. Zhang Y., et al., DNA Damage-Regulated Autophagy Modulator 1 (DRAM1) Mediates Autophagy and Apoptosis of Intestinal Epithelial Cells in Inflammatory Bowel Disease. *Dig Dis Sci*, 2020. <https://doi.org/10.1007/s10620-020-06697-2> PMID: [33184797](#)

34. West M.A., et al., Enhanced dendritic cell antigen capture via toll-like receptor-induced actin remodeling. *Science*, 2004. 305(5687): p. 1153–7. <https://doi.org/10.1126/science.1099153> PMID: 15326355
35. Gao H., et al., Autophagy Inhibition Potentiates the Anticancer Effects of a Bendamustine Derivative NL-101 in Acute T Lymphocytic Leukemia. *Biomed Res Int*, 2020. 2020: p. 1520651. <https://doi.org/10.1155/2020/1520651> PMID: 32149078
36. Feng M., et al., Regulation of the Migration of Distinct Dendritic Cell Subsets. *Front Cell Dev Biol*, 2021. 9: p. 635221. <https://doi.org/10.3389/fcell.2021.635221> PMID: 33681216
37. Audiger C. and Lesage S., FLT3 Ligand Is Dispensable for the Final Stage of Type 1 Conventional Dendritic Cell Differentiation. *J Immunol*, 2020. 205(8): p. 2117–2127. <https://doi.org/10.4049/jimmunol.2000742> PMID: 32887750
38. Sim W.J., Ahl P.J., and Connolly J.E., Metabolism Is Central to Tolerogenic Dendritic Cell Function. *Mediators Inflamm*, 2016. 2016: p. 2636701. <https://doi.org/10.1155/2016/2636701> PMID: 26980944
39. Endo S., et al., Regulation of cytotoxic T lymphocyte triggering by PIR-B on dendritic cells. *Proc Natl Acad Sci U S A*, 2008. 105(38): p. 14515–20. <https://doi.org/10.1073/pnas.0804571105> PMID: 18787130
40. Hill G.R. and Koyama M., Cytokines and costimulation in acute graft-versus-host disease. *Blood*, 2020. 136(4): p. 418–428. <https://doi.org/10.1182/blood.2019000952> PMID: 32526028
41. Ford M.L., T Cell Cosignaling Molecules in Transplantation. *Immunity*, 2016. 44(5): p. 1020–33. <https://doi.org/10.1016/j.immuni.2016.04.012> PMID: 27192567
42. Keir M.E., et al., PD-1 and its ligands in tolerance and immunity. *Annu Rev Immunol*, 2008. 26: p. 677–704. <https://doi.org/10.1146/annurev.immunol.26.021607.090331> PMID: 18173375
43. Nolte M.A., et al., Timing and tuning of CD27-CD70 interactions: the impact of signal strength in setting the balance between adaptive responses and immunopathology. *Immunol Rev*, 2009. 229(1): p. 216–31. <https://doi.org/10.1111/j.1600-065X.2009.00774.x> PMID: 19426224
44. Denoed J. and Moser M., Role of CD27/CD70 pathway of activation in immunity and tolerance. *J Leukoc Biol*, 2011. 89(2): p. 195–203. <https://doi.org/10.1189/jlb.0610351> PMID: 20699361
45. Simpson T.R., Quezada S.A., and Allison J.P., Regulation of CD4 T cell activation and effector function by inducible costimulator (ICOS). *Curr Opin Immunol*, 2010. 22(3): p. 326–32. <https://doi.org/10.1016/j.coi.2010.01.001> PMID: 20116985
46. Hanke N., et al., Dendritic cell tumor killing activity and its potential applications in cancer immunotherapy. *Crit Rev Immunol*, 2013. 33(1): p. 1–21. <https://doi.org/10.1615/critrevimmunol.2013006679> PMID: 23510023
47. Larmonier N., Bonnotte B., and Katsanis E., Cytotoxic and antigen presenting functions of T helper-1-activated dendritic cells. *Oncoimmunology*, 2012. 1(4): p. 566–568. <https://doi.org/10.4161/onci.19370> PMID: 22754789
48. Nicolas A., et al., Dendritic cells trigger tumor cell death by a nitric oxide-dependent mechanism. *J Immunol*, 2007. 179(2): p. 812–8. <https://doi.org/10.4049/jimmunol.179.2.812> PMID: 17617571
49. Fraszczak J., et al., Peroxynitrite-dependent killing of cancer cells and presentation of released tumor antigens by activated dendritic cells. *J Immunol*, 2010. 184(4): p. 1876–84. <https://doi.org/10.4049/jimmunol.0900831> PMID: 20089706
50. Hanke N.T., et al., PIAS1 and STAT-3 impair the tumoricidal potential of IFN-gamma-stimulated mouse dendritic cells generated with IL-15. *Eur J Immunol*, 2014. 44(8): p. 2489–2499.
51. Lakomy D., et al., Cytotoxic dendritic cells generated from cancer patients. *J Immunol*, 2011. 187(5): p. 2775–82. <https://doi.org/10.4049/jimmunol.1004146> PMID: 21804019
52. Adorini L., et al., Tolerogenic dendritic cells induced by vitamin D receptor ligands enhance regulatory T cells inhibiting allograft rejection and autoimmune diseases. *J Cell Biochem*, 2003. 88(2): p. 227–33. <https://doi.org/10.1002/jcb.10340> PMID: 12520519
53. Sandner S.E., et al., Role of the programmed death-1 pathway in regulation of alloimmune responses in vivo. *J Immunol*, 2005. 174(6): p. 3408–15. <https://doi.org/10.4049/jimmunol.174.6.3408> PMID: 15749874
54. Li X.C., et al., The role of T cell apoptosis in transplantation tolerance. *Curr Opin Immunol*, 2000. 12(5): p. 522–7. [https://doi.org/10.1016/s0952-7915\(00\)00133-3](https://doi.org/10.1016/s0952-7915(00)00133-3) PMID: 11007354
55. Li X.C., et al., T cell death and transplantation tolerance. *Immunity*, 2001. 14(4): p. 407–16. [https://doi.org/10.1016/s1074-7613\(01\)00121-2](https://doi.org/10.1016/s1074-7613(01)00121-2) PMID: 11336686
56. Alpdogan O. and van den Brink M.R., Immune tolerance and transplantation. *Semin Oncol*, 2012. 39(6): p. 629–42. <https://doi.org/10.1053/j.seminoncol.2012.10.001> PMID: 23206840
57. Robinson K.A., et al., Maintaining T cell tolerance of alloantigens: Lessons from animal studies. *Am J Transplant*, 2018. 18(8): p. 1843–1856. <https://doi.org/10.1111/ajt.14984> PMID: 29939471

58. Alcantara-Hernandez M., et al., High-Dimensional Phenotypic Mapping of Human Dendritic Cells Reveals Interindividual Variation and Tissue Specialization. *Immunity*, 2017. 47(6): p. 1037–1050 e6. <https://doi.org/10.1016/j.immuni.2017.11.001> PMID: 29221729
59. Leylek R., et al., Integrated Cross-Species Analysis Identifies a Conserved Transitional Dendritic Cell Population. *Cell Rep*, 2019. 29(11): p. 3736–3750.e8. <https://doi.org/10.1016/j.celrep.2019.11.042> PMID: 31825848
60. Leylek R., et al., Chromatin Landscape Underpinning Human Dendritic Cell Heterogeneity. *Cell Rep*, 2020. 32(12): p. 108180. <https://doi.org/10.1016/j.celrep.2020.108180> PMID: 32966789
61. Merad M., et al., The dendritic cell lineage: ontogeny and function of dendritic cells and their subsets in the steady state and the inflamed setting. *Annu Rev Immunol*, 2013. 31: p. 563–604. <https://doi.org/10.1146/annurev-immunol-020711-074950> PMID: 23516985
62. Gutierrez-Martinez E., et al., Cross-Presentation of Cell-Associated Antigens by MHC Class I in Dendritic Cell Subsets. *Front Immunol*, 2015. 6: p. 363. <https://doi.org/10.3389/fimmu.2015.00363> PMID: 26236315